J. Biochem. 121, 835-841 (1997)

# Subunit Association and Monomer Structure of CINC/Gro Revealed by $^1$H-NMR

**Hiroyuki Hanzawa,* Hideyuki Haruyama,*,[1] Kiyoshi Konishi,† Kazuyoshi Watanabe,‡ and Susumu Tsurufuji‡**

*Analytical and Metabolic Research Laboratories, Sankyo Co., Ltd., 2-58, Hiromachi 1-chome, Shinagawa-ku, Tokyo 140; †Department of Biochemistry, Toyama Medical and Pharmaceutical University Faculty of Medicine, Sugitani, Toyama 930-01; and ‡Institute of Cytosignal Research, Inc., Hiromachi, Shinagawa-ku, Tokyo 140

Received for publication, October 7, 1996

**Rat CINC/Gro is a 72 residue chemotactic factor of neutrophils, and a member of the CXC chemokine family, that includes IL-8 and MGSA/GRO. Although the three-dimensional structure of CINC/Gro had previously been determined to be that of a dimer with 200 mM NaCl, it was shown on both ultracentrifugation analysis and $^1$H-NMR spectral analysis that CINC/Gro exists mainly as a monomer at a physiological concentration, similar to other proteins belonging to this family. By reducing the NaCl concentration, the equilibrium could be shifted to the monomer, making it possible to observe the monomer and dimer resonances in $^1$H-NMR spectra. There were no significant chemical shift changes of $\alpha$ protons in the $\beta$ sheet between the monomer and dimer, suggesting that the $\beta$ sheet structure was retained in the monomer. Instead, the chemical shift changes of $\alpha$ protons were significant at I18 and K21, which are located in the long loop region interacting with the $\alpha$ helix, and V59 at the beginning of the $\alpha$ helix, indicating structural changes in the relative positions of the $\alpha$ helix and $\beta$ sheet.**

**Key words: chemical shift, equilibrium, IL-8 family, NMR.**

CINC/Gro is a chemotactic factor produced by rat renal epithelial cells and normal rat kidney epithelial cell line NRK-52E stimulated by lipopolysaccharides, tumor necrosis factor-$\alpha$ and interleukin 1$\beta$ (*1*). Since CINC/Gro preferentially attracts neutrophils and the first of its four conserved cysteine residues is separated by an intervening amino acid (C-X-C), CINC/Gro is classified into the CXC chemokine family, that includes IL-8 and MGSA/Gro. CINC/Gro is considered to be the rat counterpart of human MGSA/Gro because of the high sequence homology (74% sequence identity) (*2*).

In the course of our structural study of CINC/Gro, the appearance of the $^1$H-NMR spectrum was found to be rather complicated at a low salt concentration, suggesting the presence of a monomer-dimer equilibrium.

Accordingly, homonuclear 3D NMR analysis of CINC/Gro was carried out at pH 5.3 and 40°C with 200 mM NaCl so as to keep the spectral appearance simple (*3*). Under these conditions, the three-dimensional structure of CINC/Gro was determined to be that of a homo dimer. Common to other members of the CXC chemokine family, for which the three-dimensional structures have been determined by X-ray crystallography and/or NMR spectroscopy, the monomer consists of a three-stranded $\beta$ sheet and a C-terminal $\alpha$ helix (*4, 5*). The dimer interface is formed by the $\beta$ strand of each monomer and the C termini of the $\alpha$ helices on the $\beta$ sheet of the opposite monomer.

However, other members of this family, IL-8 and MGSA/Gro, were determined to be stable dimers in the absence of salt or with lower concentrations of salt at a similar pH and temperature. The three-dimensional structure of human IL-8 was determined as a dimer at pH 5.2 and 40°C with no salt. Human MGSA/Gro is also dimeric with 45 mM potassium phosphate at pH 5.5 (*6, 7*).

On the other hand, a recent report claimed that chemically modified IL-8, which could not form a dimer, still retained full *in vitro* biological activity (*11*), indicating that the monomeric form of IL-8 is the active entity. Investigation of the monomer-dimer equilibrium by means of analytical ultracentrifugation and cross-linking experiments showed that the IL-8 monomer is dominant at nanomolar concentrations where IL-8 is active as a chemotactic factor (*12-15*).

In CINC/Gro, the monomer-dimer equilibrium was assumed to be shifted to the monomer state under low ionic conditions, unlike in the cases of IL-8 and human MGSA/Gro. In the case of human platelet factor-4, another member of the CXC chemokine family, a monomer-dimer-tetramer equilibrium was observed on $^1$H-NMR. Its association mechanism has been studied using well resolved ring proton resonances (*8-10*), but PF4 does not exhibit activity as a chemoattractant.

Thus, analysis of the monomer-dimer equilibrium of CINC/Gro is expected to afford valuable information on not only the physicochemical nature of the protein association but also the intact structure of CXC chemokine in the

[1] To whom correspondence should be addressed. Tel: +81-3-3492-3131, Fax: +81-3-5436-8567

Abbreviations: CINC, cytokine-induced neutrophil chemoattractant; MGSA, melanoma growth-stimulating activity; HOHAHA, homonuclear Hartman-Hahn spectroscopy; NMR, nuclear magnetic resonance; NOESY, nuclear Overhauser enhancement spectroscopy.

monomer state. At the present stage, the biological significance of the dimeric state is not clear. However, detailed analysis of this phenomenon is expected to help answer this question.

Here, we describe that rat CINC/Gro exists under a monomer-dimer equilibrium, especially under low ionic conditions, and try to answer the question of why subunit associations become weaker from structural and thermodynamical points of view. Utilizing the fact that the monomer and dimer structures could be monitored by $^1$H-NMR, the structural changes between the monomer and the dimer are discussed based on the results of chemical shift analysis.

## MATERIALS AND METHODS

The expression and purification of recombinant CINC/Gro from *Escherichia coli* were performed as described previously except that prior to the reverse phase high performance chromatography, cation exchange chromatography on a CM-Sepharose column equilibrated at pH 7.5 with a NaCl gradient (0 to 0.5 M) was performed (*16*). Samples were lyophilized and dissolved in 100% $D_2O$ or 90% $H_2O$–10% $D_2O$. The pH was measured with a pH-meter that had been calibrated with pH standards, and correction for the isotope effect was performed taking pH = pH (direct reading) − 0.4 in the case of 100% $D_2O$ (*17*).

$^1$H-NMR experiments were performed with a JEOL GSX500 spectrometer. All 2D spectra were collected over 2,048 points along $t_2$ and 256 increments along $t_1$, and quadrature detection was achieved with the method of States *et al.* (*18*). The solvent resonance of HOD or $H_2O$ was suppressed by selective irradiation with DANTE pulses during the relaxation delay. 2D Homonuclear Hartman Hahn spectra were recorded with a 45 ms MLEV-17 mixing scheme (*19*). NOESY spectra were recorded with a mixing time of 150 ms (*20*).

Data processing was carried out with NMR1 or NMR2 software on a DEC station 5000/200 computer. 2D spectra were processed using a shifted sine bell function and zero filled to 2K × 2K points in both dimensions.

Sedimentation equilibrium experiments were carried out with a Beckman analytical ultracentrifuge, OPTIMA X-LA. CINC/Gro at 0.025 mM in 20 mM Tris-HCl, pH 5.0, was centrifuged at 22,000 rpm. The resulting absorbance gradients at 225 nm were fitted to a single ideal species:

$$A_r = A_0 \exp[H \times M(r^2 - r_0^2)] + E$$

or a monomer-dimer associating system:

$$A_r = A_0 \exp[H \times M(r^2 - r_0^2)] + A_0^2 K_a \exp[H \times M^*2(r^2 - r_0^2)] + E$$

where $A_r$ and $A_0$ are the absorbance values at $r$ and $r_0$, respectively, and

$$H = [(1 - \nu\rho) \times \omega^2]/2RT$$

where $\nu$ is the partial specific volume, $\rho$ the solvent density, $\omega$ the angular velocity in radians/s, $R$ the universal gas constant, $T$ the absolute temperature, $K_a$ the association constant, $M$ the molecular weight of the monomer, and $E$ the baseline offset. The partial specific volume, 0.72, of this protein, was calculated from the amino acid sequence (*21*).

## RESULTS

*Aggregation State of CINC/Gro*—Figure 1a shows the amide region of the HOHAHA spectrum obtained at pH 5.3 in the absence of NaCl. For Ala 42, two amide resonances were observed at 9.55 and 9.68 ppm, which correlate with the same chemical shifts of $\beta$ protons. Similar paired amide resonance was observed for Cys 11 and several other residues. Too many amide resonances hampered the assignment under these solution conditions. Exploring other conditions, it was found that an increased NaCl concentration (200 mM, Fig. 1b) made each amide proton coalesce to one resonance. For this reason, the three-dimensional structure of CINC/Gro was determined at pH 5.3 with 200 mM NaCl (*3*).

Furthermore, in the NH-NH region of the HOHAHA spectrum without NaCl (Fig. 1b), cross peaks were observed between the paired amide resonances. Since these cross peaks were also observed in the NOESY spectrum (data not shown), they could be assigned to the exchange signals connecting the two states on equilibrium. The distribution of the paired NH resonances over the protein indicated that these spectral changes can not be explained by a local conformational change.

Figure 2, a–d, shows the aromatic region of CINC/Gro at

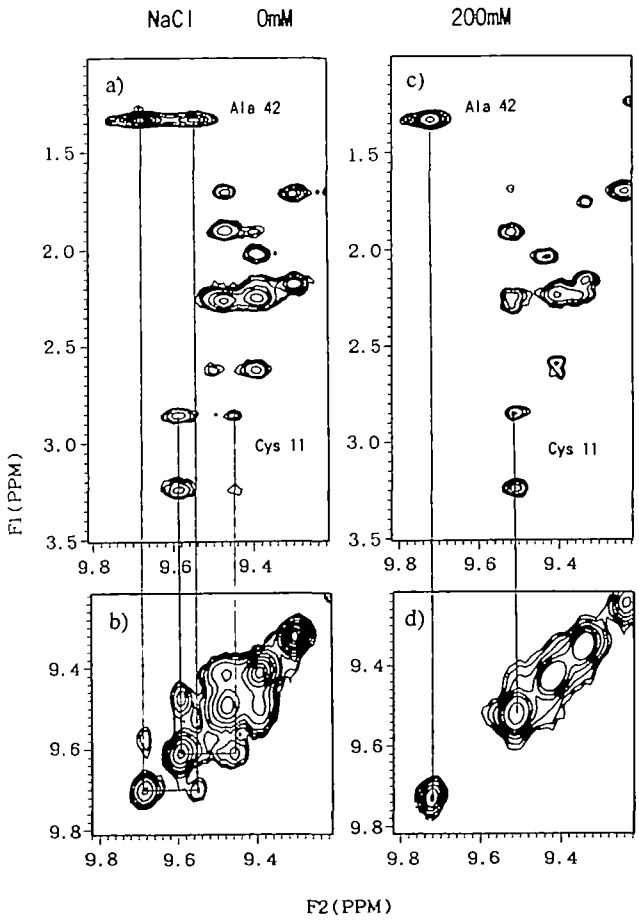


**Fig. 1. HOHAHA spectra of CINC/Gro at 40°C without NaCl (a) and (b), and with 200 mM NaCl (c) and (d).** The protein concentration was 2 mM, and no buffer was used.

various CINC/Gro concentrations at pH 5.7 and 40°C without NaCl. Out of the three aromatic residues, His 19, Phe 20, and His 34, the C2 proton resonances of His 19 and His 34 were observed as well isolated singlets, as shown in Fig. 2a. In the HOHAHA spectrum recorded at this concentration (Fig. 2e), several residues including Ala 42, which afforded the paired amide resonances at the lower concentration, gave single amide resonances. On lowering of the CINC/Gro concentration from 5.8 to 0.7 mM, the single resonance of the C2 proton of His 34 split into two resonances. These concentration-dependent spectral changes were essentially the same as those observed with varying NaCl concentrations, and indicated that CINC/Gro exists under aggregation equilibrium, monomer-dimer equilibrium in this case. The monomer population should increase as the protein concentration decreases, thus the lower field resonance which appeared at 2.9 mM and gradually increased at 1.4 and 0.7 mM was assigned as the monomer resonance, and the high field resonance was assigned to the dimer, as shown in Fig. 2.

*Analytical Ultracentrifugation Experiments and Association Constants*—Ultracentrifugation was performed to assess the state of aggregation under the present experimental conditions. Figure 3 shows the absorbance gradient at 225 nm in centrifuged cells for CINC/Gro after sedimentation equilibrium was attained. When the absorbance gradients were fitted to a single ideal species, the apparent molecular weight was 8,500 in the absence of NaCl. This is slightly larger than 7,800, the molecular weight of monomer CINC/Gro calculated from its chemical formula. The increased apparent molecular weight suggested the coexistence of both the monomer and the dimer. With 200 mM NaCl, the apparent molecular weight increased to 11,000, indicating that the dimer population increased on the addition of NaCl. Judging from this result, the change seen in the NMR spectra accompanying NaCl addition was ascribed to a shift in the population to the dimer.

The equilibrium constant for the association is defined as $K_a = [D]/[M]^2\ M^{-1}$, where D stands for the dimer and M for the monomer. $K_a$ was estimated by fitting the absorbance gradients to monomer-dimer associating systems, and was determined to be $1.3 \pm 0.3 \times 10^3\ M^{-1}$ without NaCl and $1.7 \pm 0.1 \times 10^4\ M^{-1}$ with 200 mM NaCl.

Since the two resonances ascribed to the monomer and dimer states were separated in $^1$H-NMR spectra, as shown in Fig. 2, the dimer and monomer populations could be obtained by the integration of $^1$H-NMR resonances. Using the C2 resonances of His 34, the monomer state being assigned to the low field resonance and the dimer state to the high field resonance, an association constant of $K_a = 2.3 \times 10^3\ M^{-1}$ was obtained at pH 5.0 without NaCl. This value was in relatively good agreement with the $K_a$ ob-

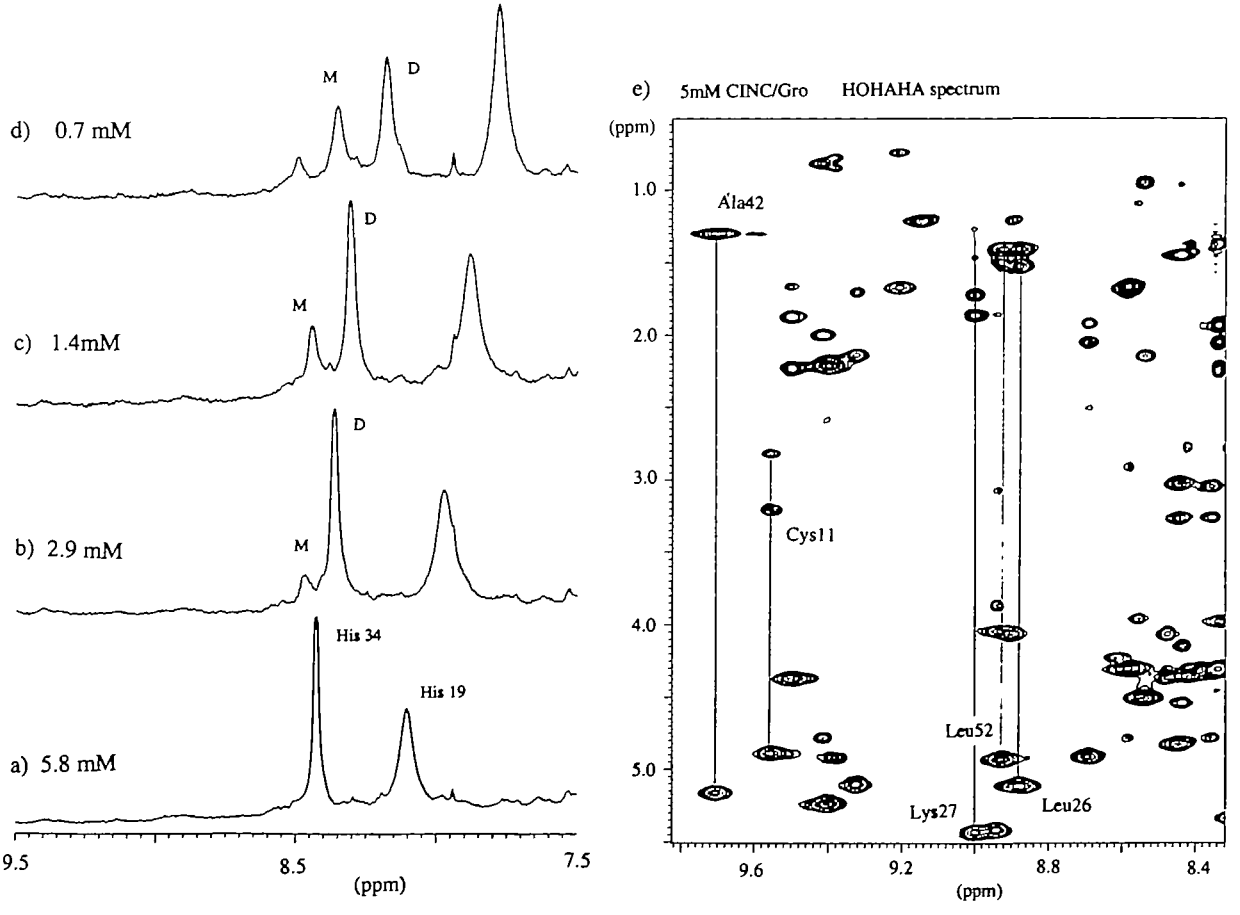


Fig. 2. **Effects of concentration on the CINC/Gro C2 proton resonances of His 19 and His 34 (a-d), and amide protons (e).** A series of $^1$H-NMR spectra were recorded with different CINC/Gro concentrations as indicated in the figure, at pH 5.7 (a-d) and pH 5.3 (e), at 40°C without NaCl.

tained on ultracentrifugation, taking into account the difference in the solvent conditions, *i.e.* 20 mM Tris-HCl was used for ultracentrifugation but no buffer was used for NMR.

*pH and Temperature Effects on the Equilibrium*—Figure 4 shows the aromatic region of $^1$H-NMR spectra of 1.4 mM CINC/Gro at various pHs. At pH 5.6, the resonances of the C2 proton of His 34 in both the monomer and dimer states were clearly observed. With increasing pH, the monomer resonances became smaller, and were finally negligible at pH 6.8. On the other hand, decreasing pH made the monomer resonances larger, and chemical shift differences between the monomer and dimer resonances smaller, until they coalesced at pH 4.3. Similar pH dependency was shown by the appearance of amide resonances of Ala 42 and several other residues, apart from the equilibrium shift to dimer formation due to the higher concentration (5 mM CINC/Gro) employed for recording HOHAHA spectra (Figs. 2e and 5a).

The temperature dependence of the monomer-dimer population was elucidated from the integrated intensities of the His 34 C-2 proton at 20, 30, 40, and 50°C (data not shown). The natural logarithm of $K_a$ was plotted *versus* the inverse temperature in Kelvin (van't Hoff plot). From the slopes of the least-squared fitted lines, enthalpy values, $\Delta H$, were obtained. The Gibbs free energy of association was directly calculated from the equilibrium constant. The entropic contribution, $\Delta S$, was calculated using $\Delta S = (\Delta H - \Delta G)/T$. The thermodynamic parameters for dimer formation were estimated to be as follows: $\Delta H = -8.3$ kcal/mol, $\Delta G = -5.3$ kcal/mol, and $\Delta S = -9.9$ eu (at 30°C).

*Chemical Shift Differences between the Monomer and the Dimer*—$^1$H-NMR assignments at pH 3.3 without NaCl at 5 mM CINC/Gro were performed with reference to the assignments at pH 5.3 with 200 mM NaCl. Figure 5a shows an example of the NH-$\alpha$H region of the HOHAHA spectrum. Since no significant chemical shift changes of the $\alpha$ and sidechain protons were observed for most residues, the paired NH resonances could be easily identified. The exchange cross peaks observed in the HOHAHA spectra also facilitated assignments. Figure 5b summarizes the chemical shift differences of the amide and $\alpha$ protons between the monomer and the dimer. For the residues which gave only one NH-$\alpha$H cross peak, the chemical shift differences between paired resonances were set at zero. For the amide protons, chemical shift changes which exceeded 0.3 ppm (chosen arbitrarily) were observed for Leu 26, Lys 27, Val 28, Ile 41, Gln 60, Ile 62, and Leu 67. These residues are located in the $\beta$ sheet or $\alpha$ helix. Significant chemical shift changes of $\alpha$ protons greater than 0.1 ppm were only observed for three residues, Ile 18, Lys 21, and Val 59. The positions of these residues in CINC/Gro are shown in Fig. 6.

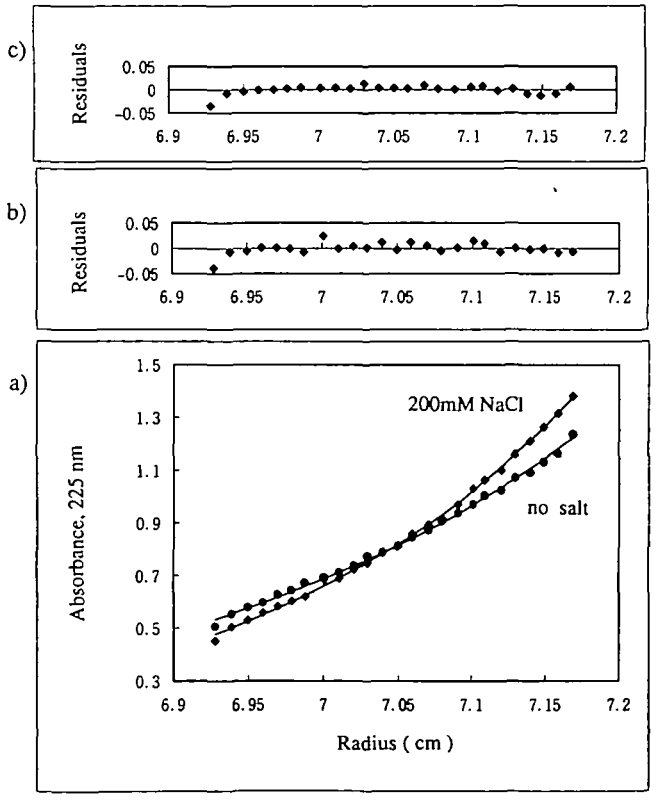


Fig. 3. **Molecular weight determination of CINC/Gro by analytical ultracentrifugation.** (a) The absorbance gradients at 225 nm in centrifuged cell without NaCl and with 200 mM NaCl were fitted to an equation describing a monomer-dimer association. The residuals of the best curve are shown in (b) without NaCl and (c) with 200 mM NaCl. The other solution conditions were the same (pH 5.0, 20 mM Tris-HCl). The initial concentration of CINC/Gro was 0.025 mM.

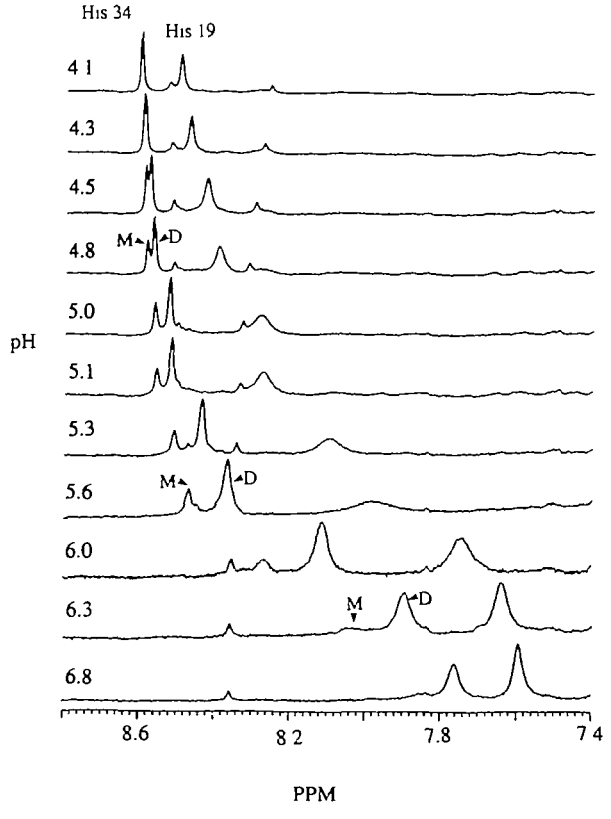


Fig. 4. **Effect of pH on the CINC/Gro C2 proton resonances of His 19 and His 34.** $^1$H-NMR spectra of CINC/Gro were obtained at 40°C. The CINC/Gro concentration was 1.4 mM without NaCl.

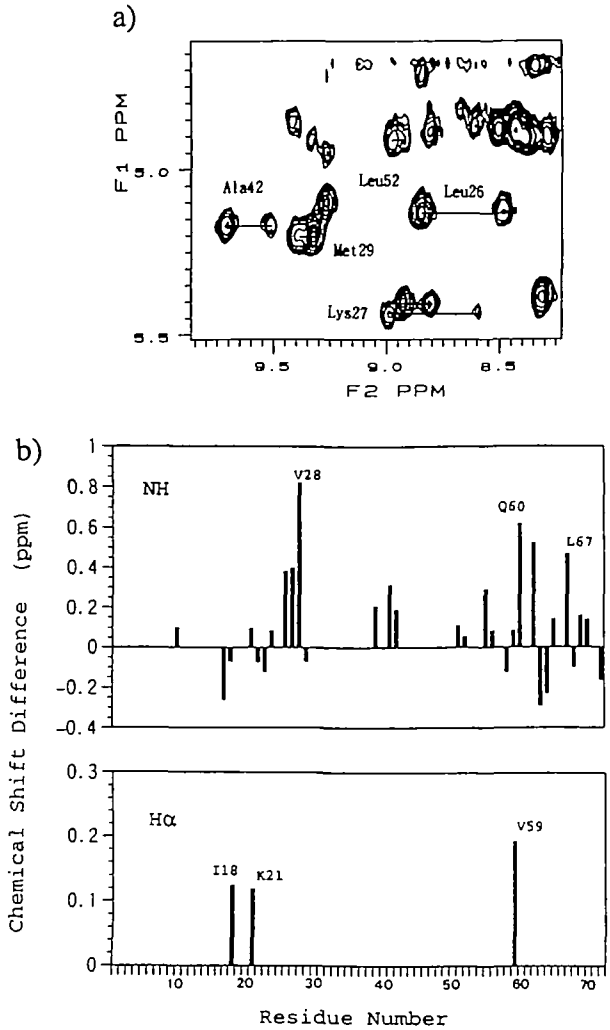


Fig. 5. **(a) An example of the NH-αH region of a HOHAHA spectrum without NaCl at pH 3.3.** For Ala 42, Met 29, Leu 26, Leu 52, and Lys 27, paired amide resonances with the same chemical shifts of $\alpha$ protons were observed. **(b) The chemical shift differences of amide and $\alpha$ protons between the monomer and the dimer.** The value of $\Delta\delta$ was calculated as $\Delta\delta = \delta(\text{dimer}) - \delta(\text{monomer})$.

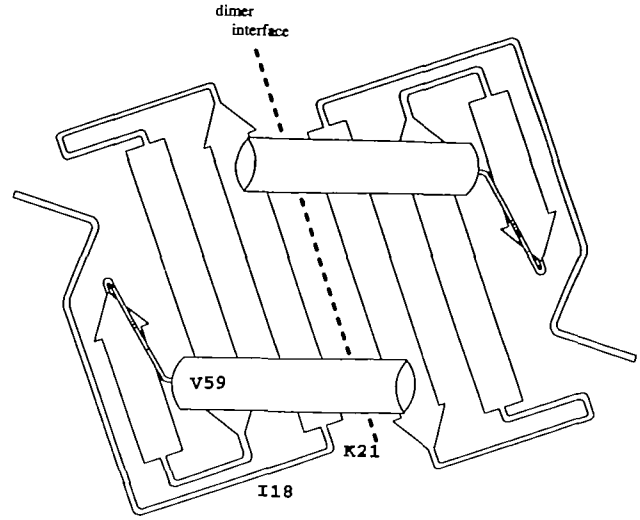


Fig. 6. **Schematic drawing of the CINC/Gro secondary structure with the locations of Ile 18, Lys 21, and Val 59.** Significant chemical shift differences of $\alpha$ protons between the monomer and the dimer were observed at pH 3.3 and 40°C.

## DISCUSSION

In this study, CINC/Gro was found to exist in monomer-dimer equilibrium. Under low ionic conditions the monomer and dimer could be separately monitored by $^1$H-NMR. Protein-protein associations are involved in many biological phenomena. The analysis of these processes on an atomic basis is important in structural biology. CINC/Gro is an ideal model system for studying dimer formation at the atomic level, because it is a small protein with complete $^1$H-NMR assignments, and its equilibrium can be controlled by means of pH and the salt concentration in the protein concentration range suitable for NMR spectroscopy. From the biological point of view, the monomer is the probable functional form of CINC/Gro. Thus, information on the monomer structure constitutes a clue for understanding the binding of CINC/Gro to its receptor.

Inter-subunit interactions in CINC/Gro at pH 5.2 were strengthened by the addition of 200 mM NaCl, suggesting that hydrophobic interactions or unfavorable repulsive interactions of like-charges are involved in the association process. Along the interfaces of subunits, Lys 27 is found at the center of the $\beta$ strand facing the other subunit. This unfavorable repulsive charge interaction may be the main factor causing the ionic strength-dependent dimer formation, although the contributions of other factors cannot be ignored.

Generally, the driving forces for protein association can be classified according to thermodynamic parameters. The negative enthalpy and entropy observed in CINC/Gro indicate that the subunit association is driven by hydrogen-bonding and van der Waals interactions (*22, 23*). This reflects the structural features of CINC/Gro in that four hydrogen bonds are formed between the intersubunit antiparallel $\beta$ sheets.

In the pH titration experiments, it was observed that the monomer-dimer equilibrium was affected between pH 3 and 6. This may imply that acidic residues or His residues are directly involved in the intersubunit interaction. As judged on reference to the three-dimensional structure of CINC/Gro, the side chain of Glu 55 extends toward the other subunit and can interact with the side chain of Lys 68, although, at present, there is no evidence to support this salt bridge formation.

A structural study on the human IL-8 dimer was performed at pH 5.2 without NaCl (*5*), while the monomer of CINC/Gro was present at pH 5.3 without NaCl. Human MGSA exists as a dimer at pH 5.5 with 50 mM potassium phosphate (*6*). Clearly, the strength of dimer formation of CINC/Gro is weaker than that in the cases of human IL-8 and MGSA at comparable protein concentrations and under comparable solution conditions. This can be ascribed to the differences between the secondary structures of these proteins. The number of intersubunit hydrogen bonds is 6 in IL-8 and MGSA, while there are 4 in CINC/Gro. This is due to the existence of Pro 30 at the edge of the $\beta$ strand in

CINC/Gro. The amide proton of the corresponding residue, Glu 29 in IL-8 and Ser 30 in MGSA, can participate in intersubunit hydrogen bonding to strengthen the intersubunit interaction. This is consistent with the results of thermodynamical analysis that indicated the major driving force for protein association is inter-subunit hydrogen bonding.

In the $\beta$ sheet comprising the interface, no chemical shift changes of the $\alpha$ protons were observed between the monomer and the dimer. Since chemical shifts of the $\alpha$ protons have been shown to correlate with the secondary structure, this suggests that the $\beta$ sheet structure is retained in the monomer.

On the other hand, amide proton chemical shift changes were observed for many residues. Based upon the relationship between amide proton chemical shifts and hydrogen bond strength (*24*), the main factor for amide proton chemical shift changes in the $\beta$ sheet region could be the changes in hydrogen bond strength. In the three-stranded $\beta$ sheet, the largest chemical shift changes were observed for Leu 26 and Val 28, where hydrogen bonds are lost on subunit dissociation, while small differences were observed for Cys 51 and Leu 52, which are located in a $\beta$ strand distant from the interface.

Recently, the three-dimensional structure of a monomeric IL-8 analog [IL-8(4-72) Leu25→$NCH_3$] was reported (*26*). In the monomeric analog, the triple-stranded $\beta$ sheet is retained, however, the C terminal 6 residues are disordered where they are helical in the dimer. In the $\alpha$ helix of CINC/gro, the chemical shift changes of $\alpha$ protons between the dimer and the monomer were not significant, although amide protons showed large chemical shift differences. This suggested that drastic structural changes might not occur in the $\alpha$ helix of CINC/Gro.

Among the three residues of which the $\alpha$ protons exhibited large chemical shift changes, Val 59 is located at the beginning of the $\alpha$ helix, and Ile 18 and Lys 21 in the loop region interacting with the $\alpha$ helix. In the dimer structure, the C terminal of the $\alpha$ helix lies on the $\beta$ sheet of the other subunit, and the $\alpha$ helices of the two subunits interact with each other. The observed chemical shift changes of $\alpha$ protons may correspond to the shift in the position of the $\alpha$ helix. The relative position of the $\alpha$ helix as to the $\beta$ sheet can change easily in the association/dissociation process.

The loops where Ile 18 and Lys 21 are located correspond to those of human IL-8, in which chemical shift changes were observed for some residues when bound to an N-terminal peptide of the IL-8 receptor (*25*). It is interesting to note that the same loop may be perturbed by both dissociation into the monomer and binding to the receptor.

For more detailed comparison of the monomer and dimer structures, isotope-labeled CINC/Gro has been prepared and further analysis is in progress.

We wish to thank J. Inoue, T. Ritani, and M. Koizumi of Beckman Instruments Ltd. for performing the analytical ultracentrifugation.

## REFERENCES

1. Watanabe, K., Kinoshita, S., and Nakagawa, H. (1989) Purification and characterization of cytokine-induced neutrophil chemoattractant produced by epithelioid cell line of normal rat kidney (NRK-52E cell). *Biochem. Biophys. Res. Commun.* **161**, 1093-1099
2. Watanabe, K., Konishi, K., Fujioka, M., Kinoshita, S., and Nakagawa, H. (1989) The neutrophil chemoattractant produced by rat kidney epithelioid cell line NRK-52E is a protein related to the KC/gro protein. *J. Biol. Chem.* **264**, 19559-19563
3. Hanzawa, H., Haruyama, H., Watanabe, K., and Tsuruhuji, S. (1994) The three-dimensional structure of rat cytokine CINC/Gro in solution by homonuclear 3D NMR. *FEBS Lett.* **354**, 207-212
4. St. Charles, R., Walz, D.A., and Edward, B.F.P (1989) The three-dimensional structure of bovine platelet factor 4 at 3.0 Å resolution. *J. Biol. Chem.* **264**, 2092-2099
5. Clore, B.M., Appella, E., Yamada, M., Matsushima, K., and Gronenborn, A.M. (1990) Three-dimensional structure of interleukin-8 in solution. *Biochemistry* **29**, 1689-1696
6. Fairbrother, W.J., Reilly, D., Colby, T.J., Hesselgesser, J., and Horuk, R. (1994) The solution structure of melanoma growth stimulating activity. *J. Mol. Biol.* **243**, 252-270
7. Kim, K.S., Clark-Lewis, I., and Sykes, B.D. (1994) Solution structure of GRO/melanoma growth stimulating activity determined by $^1$H-NMR spectroscopy. *J. Biol. Chem.* **269**, 32909-32915
8. Mayo, K.H. and Chen, M.J. (1989) Human platelet factor 4 monomer-dimer-tetramer equilibria investigated by $^1$H-NMR spectroscopy. *Biochemistry* **28**, 9469-9478
9. Mayo, K.H. (1991) Low-affinity platelet factor 4 $^1$H NMR derived aggregate equilibria indicate a physiological preference for monomers over dimers and tetramers. *Biochemistry* **30**, 925-934
10. Chen, M.J. and Mayo, K.H. (1991) Human platelet factor 4 subunit association/dissociation thermodynamics and kinetics. *Biochemistry* **30**, 6402-6411
11. Rajarathnam, K., Sykes, B.D., Kay, C.M., Dewald, B., Geiser, T., Baggiolini, M., and Clark-Lewis, I. (1994) Neutrophil activation by monomeric interleukin-8. *Science* **264**, 90-92
12. Burrows, S.D., Doyle, M.L., Murphy, K.P., Franklin, S.G., White, J.R., Brooks, I., McNulty, D.E., Scott, M.O., Knutson, J.R., Porter, D., Young, P.R., and Hensley, P. (1994) Determination of the monomer-dimer equilibrium of interleukin-8 reveals it is a monomer at physiological concentrations. *Biochemistry* **33**, 12741-12745
13. Schnitzel, W., Monschein, U., and Besemer, J. (1994) Monomer-dimer equilibria of interleukin-8 and neutrophil-activating peptide 2. Evidence for IL-8 binding as a dimer and oligomer to IL-8 receptor B. *J. Leuko. Biol.* **55**, 763-770
14. Clark-Lewis, I., Schumacher, C., Baggiolini, M., and Benhard, M. (1991) Structure-activity relationship of interleukin-8 determined using chemically synthesized analogs. *J. Biol. Chem.* **266**, 23128-23134
15. Hebert, C.A., Vitangcol, R.V., and Baker, J.B. (1991) Scanning mutagenesis of interleukin-8 identifies a cluster of residues required for receptor binding. *J. Biol. Chem.* **266**, 18989-18994
16. Konishi, K., Takata, Y., Watanabe, K., Date, Y., Yamamoto, M., Murase, M., Yoshida, H., Suzuki, T., Tsurufuji, S., and Fujioka, M. (1993) Recombinant expression of rat and human gro protein in *Escherichia coli*. *Cytokine* **5**, 506-511
17. Glasoe, P.K. and Long, F.A. (1960) Use of glass electrodes to measure acidities in deuterium oxide. *J. Phys. Chem.* **64**, 188-190
18. States, D.J., Habercorn, R.A., and Ruben, D.J. (1982) A two-dimensional nuclear Overhauser experiment with pure absorption phase in four quadrants. *J. Magn. Reson.* **48**, 286-292
19. Bax, A. and Davis, D.G. (1985) Mlev-17-based two-dimensional homonuclear magnetization transfer spectroscopy. *J. Magn. Reson.* **65**, 355-360
20. Jeener, J., Meier, B.H., Bachmann, P., and Ernst, R.R. (1979) Investigation of exchange process by two-dimensional NMR spectroscopy. *J. Chem. Phys.* **71**, 4546-4553
21. Cohn, E.J. and Edsall, J.T. (1943) *Proteins, Amino Acids and Peptides as Ions and Dipolar Ions*, p. 157, Rheinhold, New York
22. Klotz, I.M. (1973) Physicochemical aspects of drug-protein interactions: a general perspective. *Ann. N.Y. Acad. Sci.* **226**, 18-24

23. Ross, P.D. and Subramanian, S. (1981) Thermodynamics of protein association reactions: forces contributing to stability. *Biochemistry* **20**, 3096-3102
24. Wishart, D.S., Sykes, B.D., and Richards, F.M. (1991) Relationship between nuclear magnetic resonance chemical shifts and protein secondary structure. *J. Mol. Biol.* **222**, 311-333
25. Clubb, R.T., Omichinski, J.G., Clore, G.M., and Gronenborn, A.M. (1994) Mapping the binding surface of interleukin-8 complexed with an N-terminal fragment of the type 1 human interleukin receptor. *FEBS Lett.* **338**, 93-97
26. Rajarathnam, K., Clark-Lewis, I., and Sykes, B.D. (1995) $^1$H-NMR solution structure of an active monomeric interleukin 8. *Biochemistry* **34**, 12983-12990